AGU PUBLICATIONS

JGR

Journal of Geophysical Research: Oceans

RESEARCH ARTICLE

10.1002/2014JC010580

Key Points:
- Multiple platforms capture biogeochemical response to intense upwelling
- Phytoplankton response is greatest only after intense upwelling ceases
- Projected sustained upwelling has implications for CO_2 uptake on this shelf

Correspondence to:
W. Evans,
wiley.evans@noaa.gov

Citation:
Evans, W., B. Hales, P. G. Strutton, R. K. Shearman, and J. A. Barth (2015), Failure to bloom: Intense upwelling results in negligible phytoplankton response and prolonged CO_2 outgassing over the Oregon shelf, *J. Geophys. Res. Oceans*, *120*, 1446–1461, doi:10.1002/2014JC010580.

Received 14 NOV 2014
Accepted 21 JAN 2015
Accepted article online 27 JAN 2015
Published online 5 MAR 2015

Failure to bloom: Intense upwelling results in negligible phytoplankton response and prolonged CO_2 outgassing over the Oregon shelf

Wiley Evans[1,2], Burke Hales[3], Peter G. Strutton[4], R. Kipp Shearman[3], and John A. Barth[3]

[1]Pacific Marine Environmental Laboratory, National Oceanic and Atmospheric Administration, Seattle, Washington, USA, [2]Ocean Acidification Research Center, School of Fisheries and Ocean Sciences, University of Alaska Fairbanks, Fairbanks, Alaska, USA, [3]College of Earth, Ocean, and Atmospheric Sciences, Corvallis, Oregon, USA, [4]Institute for Marine and Antarctic Studies, University of Tasmania, Hobart, Tasmania, Australia

Abstract During summer, upwelled water with elevated CO_2 partial pressure (pCO_2) and nutrients outcrops over the Oregon (OR) inner shelf. As this water transits across the shelf, high rates of primary production fueled by the upwelled nutrients results in net atmospheric CO_2 drawdown. Upwelled source-waters typically have pCO_2 approaching 1000 μatm that is then reduced to ~200 μatm. For almost the entire month of July 2008, strong and persistent upwelling brought cold (~8°C), saline (~33.5), high-pCO_2 (>600 μatm) water to our midshelf buoy site, and high-pCO_2 water was broadly distributed over the shelf. Chlorophyll levels, as a proxy for phytoplankton biomass, were low (< 2 mg m^{-3}) on the shelf during the period of most intense upwelling, and satellite data showed no evidence of a downstream phytoplankton bloom. A small chlorophyll increase to ~4 mg m^{-3} was observed at our buoy site following a decrease in the strength of southward wind stress 10 days after upwelling initiated. Chlorophyll levels further increased to ~10 mg m^{-3} only after a cease in upwelling. These higher levels were coincident with the appearance of water masses having temperature and salinity properties distinct from recently upwelled water. We suggest that rapid offshore transport and subsequent subduction before phytoplankton populations could respond is the most likely explanation for the persistent low chlorophyll and elevated surface-water pCO_2 throughout the July upwelling event. This mechanism likely dominates under conditions of strong and persistent upwelling-favorable winds that coincide with close proximity of low-density offshore waters, which may have implications for the biogeochemical functioning of this system under future climate scenarios.

1. Introduction

The magnitude of the open ocean sink for atmospheric CO_2 is becoming well constrained [*Takahashi et al.*, 2002, 2009], but this is less true for the coastal ocean [*Borges et al.*, 2005; *Hales et al.*, 2008; *Laruelle et al.*, 2010]. In a global sense, coastal margins are regarded as a net sink for atmospheric CO_2 [*Borges*, 2005; *Borges et al.*, 2005; *Cai et al.*, 2006; *Dai et al.*, 2013; *Laruelle et al.*, 2010], but uncertainty arises because the temporal and spatial coverage of observations is limited relative to the system variability. The range of surface water pCO_2 observed in coastal oceans far exceeds that seen in the open ocean, and values change significantly on subdaily to super-annual frequencies [*Chavez et al.*, 2007; *DeGrandpre et al.*, 1997, 2002; *Evans et al.*, 2011; *Friederich et al.*, 2002; *Hales et al.*, 2005b, 2008, 2012; *Jiang et al.*, 2008]. Variable pCO_2 conditions are inherent to upwelling-dominated coastal regions, where upwelling supplies high-CO_2 water to the surface and strong biological response leads to depletion [*Borges et al.*, 2005; *Cai et al.*, 2006; *Chavez et al.*, 2007; *Hales et al.*, 2008].

The Oregon coastal margin, part of the larger Cascadian margin that extends from northern California to Vancouver Island, is seasonally upwelling-dominated and experiences highly variable upwelling conditions [*Barth et al.*, 2007; *Huyer et al.*, 2005, 2007; *Pierce et al.*, 2006]. Beginning in approximately April and ending around October, CO_2 and nutrient-rich water from depth is upwelled to the surface by equatorward winds over the shelf. The nitrate concentrations and pCO_2 levels within the upwelled source water have been observed to be ~35 μM and ~1000 μatm, respectively [*Evans et al.*, 2011; *Hales et al.*, 2005a, 2005b; *Hill and Wheeler*, 2002; *van Geen et al.*, 2000]. These waters are upwelled with abundant iron [*Chase et al.*, 2005] and

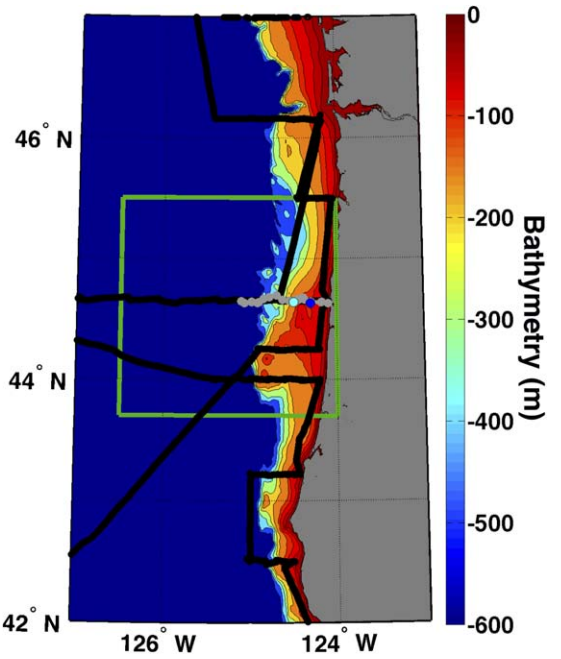

Figure 1. Map of Oregon (OR) continental margin bathymetry (color bar, m); data provided by the National Geophysical Data Center (http://www.ngdc.noaa.gov/mgg/global/global.html). Warm colors highlight the shelf (<200 m). The black line is the July 2008 cruise track of the NOAA Ship McArthur II. The blue dot is the Oregon State University (OSU) NH10 buoy position (44.633°N, 124.304°W; ~20 km from shore) and the cyan dot is the position of National Data Buoy Center (NDBC) buoy 46050 (44.641°N, 124.5°W; ~37 km from shore). MODIS satellite data were extracted for the green box for analysis using a Hovmuller diagram. Gray line is the track of an OSU Slocum glider between 17 and 21 July 2008.

preformed nutrients [*Hales et al*., 2005b], and phytoplankton assemblages in this system typically consist of fast-growing coastal diatoms [*Wetz and Wheeler*, 2003] capable of drawing high initial NO_3^- to low levels within a few days [*Dugdale et al*., 2006; *Wilkerson and Dugdale*, 1987; *Wilkerson et al*., 2006]. Upwelled waters are advected off and alongshore, fast-growing phytoplankton assemblages bloom [*Dugdale et al*., 2006; *Wetz and Wheeler*, 2003], nutrients are driven to near zero [*Hales et al*., 2005a], and pCO_2 levels are drawn down to below atmospheric values [*Hales et al*., 2005b]. This was the explanation given by *Hales et al*. [2005b] for the low observed pCO_2, but this response was not seen in July 2008.

Observations made near Newport, OR documented the occurrence of surface-water pCO_2 levels above 1000 μatm, with values in excess of 800 μatm broadly distributed over the shelf [*Evans et al*., 2011]. These high-pCO_2 waters first appeared in June 2008, during two pulses of strong upwelling-favorable winds that drove the surface exposure of deep-origin cold (~8°C), saline (~33.5) water. Following the brief June events, the shelf experienced a prolonged period of upwelling-favorable winds and high-pCO_2 conditions for most of July. The prolonged high-pCO_2 conditions had a large effect on the estimate of net annual sea-air CO_2 flux for the central OR midshelf [*Evans et al*., 2011]. Our goal here is to understand the mechanisms that limited phytoplankton community response to this upwelling, with hopes of understanding the likelihood of future events.

2. Methods

We have combined ship, mooring, satellite and glider observations to examine the response of the phytoplankton community to the July 2008 upwelling event. The ship data were collected with a system of sensors for measurement of temperature, salinity, chlorophyll fluorescence and pCO_2 in a seawater flow-through system (referred to hereafter as the OSU underway pCO_2 system). These data were collected from a single cruise from 12 to 21 July 2008 aboard the NOAA Ship *McArthur II*. This cruise began in the Columbia River estuary (46.2°N, 123.9°W) and sampled on-offshore transects southward along the OR shelf and into northern California waters, before turning north and resampling some transects, most notably the Newport Hydrographic Line (NH Line; 44.6°N; Figure 1), and ending in Seattle, Washington.

2.1. The OSU Underway pCO_2 System

The OSU underway pCO_2 system has been described in detail previously [*Evans et al*., 2011, 2012, 2013; *Hales et al*., 2004], however, some information about this system is given below. The OSU system employed a LI-COR LI-840 infrared (IR) CO_2 analyzer to detect CO_2 in a carrier gas stream equilibrated with seawater from the shipboard flow-through system. Seawater was delivered to a miniature membrane contactor (Liqui-Cel 1 × 5.5) at ~300 ml min^{-1}, and prefiltration was achieved using a custom tangential flow filter, in which 1–10% of the main flow was directed radially through an 8 μm screen to the membrane contactor. Airflow through the equilibrator was fixed at 30 ml min^{-1} and data were collected at 1 Hz. Standard sequences using gases of known CO_2 mixing ratio (xCO_2, ppm) were used to correct for IR analyzer

inaccuracy. The standards were run with atmospheric samples every 2 h. The carrier gas consisted of marine air, and no drying of the sample (seawater and atmospheric) or standard gas streams was done. Calibrated seawater xCO_2 data were adjusted to pCO_2 using the measured total equilibrator pressure, and calibrated atmospheric xCO_2 data were converted to pCO_2 using atmospheric pressure measured in the LI-COR cell. The pCO_2 system was integrated with a Seabird SBE45 for temperature and salinity, and a probe for monitoring temperature in the equilibrator. Sensors in the ship's surface-water intake provided surface seawater temperature. Equilibrator-temperature seawater pCO_2 was then corrected to pCO_2 at sea surface temperature (SST) using the difference between ship intake and equilibrator temperatures following *Takahashi et al*. [1993] and *Dickson et al*. [2007]. This correction was done after accounting for the flow-based lag time ($\sim$ 1 min) between ship's intake and equilibrator sensor locations, and was on the order of $\sim$2%.

The pCO_2 system was also integrated with a chlorophyll fluorometer (WETLabs WetStar; excitation/emission wavelengths of 460/695 nm). The seawater flow rate was monitored downstream of the pCO_2 equilibrator and used for data quality control; data from all measurements were removed during periods of low flow delivery to the equilibrator ($<$100 ml min^{-1}). All ancillary measurements were made at 1 Hz coincident with the pCO_2 measurement, and the fluorometer was kept clean during the cruise. Chlorophyll calibration of the fluorometer was described previously [*Evans et al*., 2013], but was done using extracted chlorophyll from surface Niskin bottle samples processed according to standard protocols [*Holm-Hansen*, 1978]. The intake depth for the seawater flow-through system was 3 m.

2.2. Moored Measurements

Moored observations were made at the OSU NH10 buoy, which is located $\sim$20 km from shore (about halfway between the shore and the shelf break at 200 m) directly west of Newport at the 80 m isobath (Figure 1). Moored pCO_2 measurements were made using a Submersible Autonomous Moored Instrument CO_2 sensor (SAMI-CO_2) [*DeGrandpre et al*., 1995] produced by Sunburst Sensors (http://www.sunburstsensors.com/). The SAMI-CO_2 was factory calibrated prior to deployment and positioned immediately under the surface float on the OSU NH10 buoy. In addition to the pCO_2 sensor, we deployed a Seabird SBE16plus that measured and logged temperature and salinity and recorded the signals from a SBE43 sensor for dissolved oxygen. Data from additional thermistors and salinometers positioned at select depths along the mooring line were provided by the Oregon Coastal Ocean Observing System (OrCOOS; http://agate.coas.oregonstate.edu/index.html).

We also deployed a WETLabs combination chlorophyll fluorometer and turbidity sensor (FLNTUSB which uses excitation/emission wavelengths of 470/695 nm for chlorophyll and backscatter at 700 nm for turbidity). The SBE16plus and the additional optics sensors were all positioned at approximately 1 m depth in the bridle of the buoy, adjacent to the SAMI-CO_2 sensor, and all measurements were recorded hourly. Copper tape, faceplates and shutters were used to help prevent biofouling on the FLNTUSB. We only present the chlorophyll fluorescence data here, which were calibrated using a two-point calibration curve with a zero concentration and a concentration measured from a Niskin bottle sample collected at the OSU NH10 buoy position during the July cruise. Hourly measurements of dissolved oxygen, chlorophyll fluorescence, and pCO_2 were smoothed using a 32 h running mean to reduce subdaily variability.

Dissolved oxygen values are presented here as ΔO_2, which represent the surface water concentration (μmol kg^{-1}) minus the oxygen saturation concentration (μmol kg^{-1}) at the in situ temperature and salinity. The oxygen saturation concentrations were calculated using the equations described by *García and Gordon* [1992]. To remove the effect of warming on upwelled water during the July event, we normalized our mooring pCO_2 data to a reference temperature of 7.7°C. This was the minimum 32 h running mean temperature observed in the record on 13 July 2008. The normalization of mooring pCO_2 data at SST ($pCO_{2(SST)}$) to a temperature of 7.7°C ($pCO_{2(7.7°C)}$) was done using the equation from *Takahashi et al*. [1993]. Since we normalized to the coldest observed temperatures, $pCO_{2(7.7°C)}$ will always be less than or equal to $pCO_{2(SST)}$, as the positive effect of warming due solely to decreased gas solubility has been removed.

2.3. Satellite Observations

Level 2 SST (11 μm wavelength) and chlorophyll data from the Aqua satellite's MODerate resolution Imaging Spectroradiometer (MODIS) were extracted from the NASA Ocean Color website (http://oceancolor.gsfc.nasa.gov/) for the time period 1 July to 5 August 2008. Level 2 data are swaths with 1 km resolution.

Usually there are two swaths per day, but cloud contamination inhibits satellite infrared SST and ocean color measurements. Each Level 2 file was examined to isolate the clearest cloud-free images spanning the July upwelling event. Using the clearest satellite image that revealed the greatest expanse of cold upwelled water, the SST front that separates warm offshore surface water from cold recently upwelled water near shore was defined by examining the cross-shore SST gradient in smoothed MODIS data at the latitude of the NH Line (Figure 1). A LOESS smoother with a half-power point of 0.3° of longitude was used to reduce the noise in MODIS SST data along the latitude of the NH Line (Figure 3). The isotherm that represented the front was defined as the temperature (13.2°C) and location that corresponded with the minimum SST gradient (−6.9°C (° longitude)$^{-1}$). Temporal variability in satellite chlorophyll data was also analyzed using a Hovmuller diagram created from data extracted for a box bracketing the NH Line (Figure 1). The pixels within the box were averaged for each 1 km longitude band to create a time versus longitude section.

2.4. Ancillary Data

Wind data were obtained from the National Data Buoy Center (NDBC) buoy 46050, approximately 37 km offshore (Figure 1), to illustrate the wind pattern throughout the July 2008 upwelling event. The Pacific Fisheries Environmental Laboratory (PFEL) daily and 6 hourly coastal upwelling index (http://www.pfeg.noaa.gov/products/PFEL/modeled/indices/upwelling/upwelling.html) was also used to show the intensity of upwelling during the July event relative to the 2008 upwelling season, and to aid in describing the event's progression from the initiation to the terminus of upwelling. The upwelling index used here was for 45°N, 125°W. Data from a Slocum glider that surveyed the NH Line between 17 and 12 July 2008 were acquired from the OSU glider group data archive (http://gliderfs2.coas.oregonstate.edu/gliderweb/). Archived OSU glider data consisted of temperature, salinity and pressure measurements acquired from a Seabird Glider Payload CTD, and chlorophyll fluorescence measured with a WETLabs Eco Puck. These data were collected only during glider ascents through the water column, and archived with a sample interval of ∼15 s and position information only for glider transmissions at the surface. Position was linearly interpolated in time between glider surface GPS fixes. We calculated chlorophyll from glider fluorometry using a calibration curve generated from calibrated NH10 buoy chlorophyll measurements and glider fluorometer counts collocated with the buoy observations, and the deepest (200 m) offshore fluorometer counts from the glider as the zero chlorophyll concentration endpoint.

3. Results

The daily PFEL upwelling index for 2008 showed that dominant upwelling conditions began in May, however, periods of relaxed upwelling with sporadic episodes of downwelling recurred until a 20 day span of sustained upwelling initiated in July (Figure 3). We present our results according to phases defined by characteristics in northward wind stress that bracketed this upwelling event (Figure 4). Phase 1 is the transition from northward to peak southward wind stress (−0.27 N m^{-2}), phase 2 is the period of largely sustained southward wind stress < -0.05 N m^{-2}, phase 3 is the span of weaker southward wind stress (> -0.05 N m^{-2}), and phase 4 is the period of wind stress reversals that proceeded the upwelling event that began 1 August. We include phase 4 even though continuous upwelling had ceased because, as will be shown below, the coastal ocean was still responding to the 20 days of sustained upwelling (Figure 3).

3.1. Phase 1: Transition to Peak Southward Wind Stress

Early July experienced a brief period of northward wind stress, which then transitioned to southward on 6 July and reached peak levels of −0.27 N m^{-2} by 7 July (Figure 4). Trends in SST and sea surface salinity (SSS) at NH10 followed the change in wind stress recorded at NDBC buoy 46050 (Figures 4 and 5). Prior to the wind shift on 6 July, SST at the NH10 buoy was near 14°C, but then plummeted 6 degrees C over the following 5 days (Figure 5). SSS data at NH10 showed a similar rapid change, with values initially near 30 prior to the shift in wind direction, which then increased to near 33.5 by the height of upwelling (Figure 5). MODIS chlorophyll data showed concentrations at the start of upwelling on 7 July near 3 mg m^{-3} and broadly distributed over the shelf, except in the vicinity of the Columbia River mouth where values there were above 10 mg m^{-3} (Figure 6). MODIS SST data showed cool surface water (∼11°C) only very near shore on 7 July (Figure 6). The SST front, defined as colocated with the 13.2°C isotherm by the process described above (Figure 2), was on the shelf along the NH Line with areas of 3 mg m^{-3} chlorophyll bracketing its position (Figure 6). Surface chlorophyll data recorded on the NH10 buoy confirmed the low values seen by

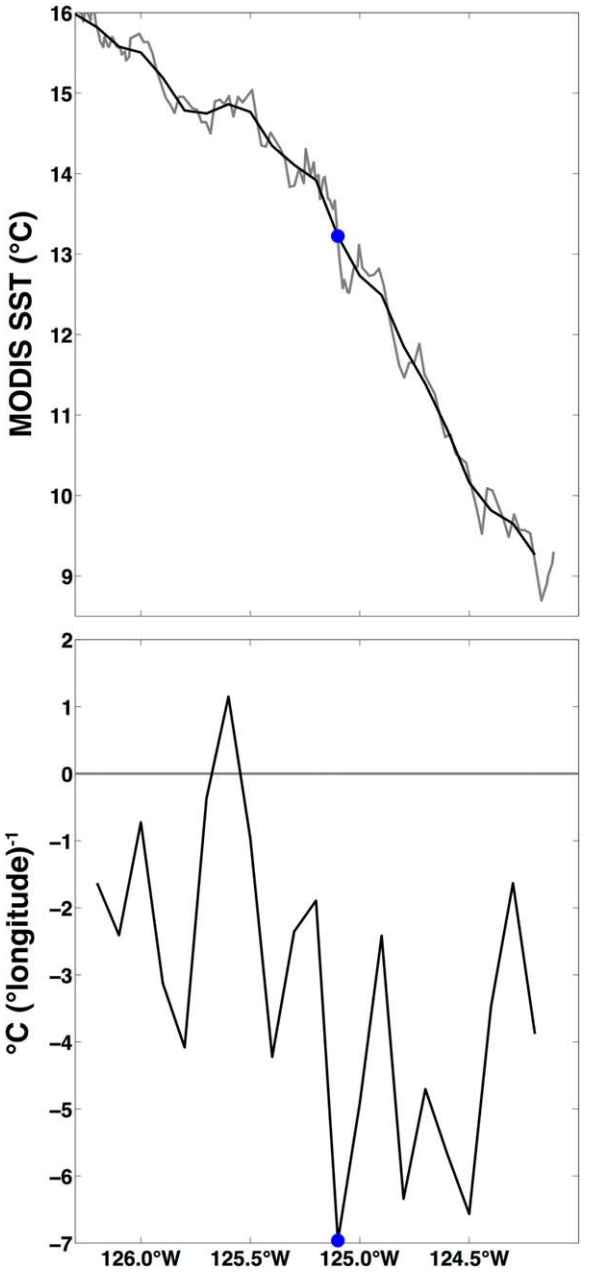

Figure 2. (top) MODIS SST (°C) and (bottom) the horizontal SST gradient (°C (°longitude) −1) along the NH Line on 12 July 2008. The SST data were smoothed using a LOESS filter with a half-power point of 0.3° of longitude. Negative values of the SST gradient indicate cooling with increasing longitude. The minimum SST gradient is where the most rapid cooling per increase in longitude took place, and was used to define the position of the offshore SST front. The minimum SST gradient (−6.9°C (°longitude)−1) and the corresponding isotherm (13.2°C) are marked with blue dots in both plots.

MODIS, with concentrations near 3 mg m^{-3} on 7 July (Figure 7). Both ΔO_2 and $pCO_{2(SST)}$ at NH10 were near equilibrium with the atmosphere at the start of upwelling on 6 July, before an extended period of very low ΔO_2 and high pCO_2 that persisted for nearly three weeks (Figure 7).

3.2. Phase 2: Sustained Southward Wind Stress < −0.05 N m^{-2}

Once southward wind stress reached −0.27 N m^{-2} on 7 July, levels < −0.05 N m^{-2} were largely sustained until 15 July (Figure 4). This 8 day phase coincided with the greatest degree of upwelling on record for 2008 (Figure 3). The coldest SSTs were observed at NH10 on 13 July (Figure 7), 6 days into the period of sustained southward wind stresses < −0.05 N m^{-2} (Figure 4). Temperatures throughout the water column at NH10 were near 8°C by 11 July (Figure 5), however, the mixed layer depth (MLD) was mostly between 10 and 30 m, as indicated by differences in potential density anomaly ($\Delta\sigma_\theta$) referenced to 2 m approaching 0.125 kg m^{-3} (Figure 5). Only on 10 and 13 July did the MLD surpass 30 m (Figure 5). MODIS SST data from 12 July revealed strong upwelling was underway, with SST close to 8°C spanning the shelf along the NH Line and the SST front nearly 20 km west of the shelf break at 44.6°N (Figure 6). The MODIS chlorophyll Hovmuller diagram revealed the offshore advection of the near 3 mg m^{-3} chlorophyll water, which was replaced with water that contained chlorophyll levels close to 1 mg m^{-3} from 7 to 15 July (Figure 8). Excluding this area of modest chlorophyll levels near 3 mg m^{-3} at the SST front, the only other area of elevated chlorophyll was in a confined patch very near shore at 44°N (Figure 6). The clear sky image of MODIS data on 12 July showed there was no evidence of a large phytoplankton bloom south of the NH Line, downstream of the area of active upwelling. This would have been expected 6 days into this phase of sustained southward wind stress < −0.05 N m^{-2} (Figure 6) had the bloom merely been translated downstream by the mean alongshore currents. Given that amount of time, an initial chlorophyll level of 1 mg m^{-3} and a conservative doubling time of 0.5 day^{-1}, a phytoplankton bloom with chlorophyll concentrations above 8 mg m^{-3} should have been visible by satellite south of the NH Line.

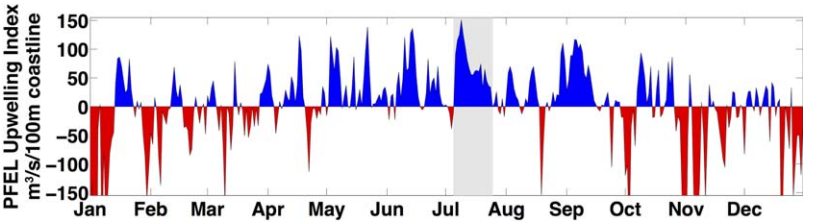

Figure 3. 2008 Pacific Fisheries Environmental Laboratory (PFEL) daily coastal upwelling index (m^3/s/100 m coastline) for the latitude of OR (45°N). The area in gray highlights a period of sustained upwelling that began 6 July and ended 25 July. The maximum daily value for 2008 (151 m3/s/100 m coastline) was reached during this period on 8 July.

The greatest increase in MODIS chlorophyll levels from those seen on 7 July was in the vicinity of the Columbia River mouth (Figure 6). Data collected aboard the NOAA Ship *McArthur II* verified the mooring and satellite observations seen during this phase of sustained southward wind stress, and showed cold (∼8°C), low-chlorophyll ($<$ 2 mg m^{-3}) water broadly distributed over the shelf near and north of the NH Line (Figure 9). Chlorophyll measured at the NH10 buoy reached minimum levels on 9 July (∼1.3 mg m^{-3}) and these low levels persisted until 12 July (Figure 7). By the end of this phase on 15 July, chlorophyll concentrations at NH10 reached 4 mg m^{-3} (Figure 7). This moderate increase in chlorophyll was the first indication of any response from the phytoplankton community at NH10 to the upwelling event, but there was no such evidence reflected in the records of ΔO_2 and pCO_2 (Figure 7). Following the steep changes in ΔO_2 and pCO_2 on 6 July, both reached plateaus on 10 July with ΔO_2 as low as -120 μmol kg^{-1} and $pCO_{2(SST)}$ as high as 800 μatm. Data collected from the ship showed pCO_2 values close to 1100 μatm over the inner shelf near shore at 44.6°N (Figure 9). The high-pCO_2 inner shelf water appeared at the mooring site on 15 July, at the terminus of this phase of sustained southward wind stress < -0.05 N m^{-2} (Figure 7). ΔO_2 data from NH10 showed no change that coincided with this increase in pCO_2 (Figure 7).

3.3. Phase 3: Weaker Southward Wind Stress

Southward wind stress abated on 15 July to weaker levels > -0.05 N m^{-2} through 25 July (Figure 4). SST began to rise at NH10 on 15 July, with values increasing from ∼ 8°C to close to 11°C by 24 July, although SST fluctuated between these two temperatures over this time period (Figure 5). Satellite SST data showed that surface water had generally warmed to 11°C ooin the vicinity of the NH Line by 23 July, but the SST front remained off the shelf although with a more irregular pattern than what was seen on 12 July (Figure 6). MODIS Chlorophyll concentrations inshore of the SST front and south of Newport had increased on 23 July from those seen in the previous clear image on 12 July, but with a patchy distribution and levels ranging from 1 to 10 mg m^{-3} (Figure 6). The Hovmuller diagram indicated chlorophyll had increased on 22 July from the low levels seen during phase 2 over the shelf, although MODIS retrievals were heavily cloud-contaminated between 15 and 22 July (Figure 8). Chlorophyll data from NH10 were generally static with levels close to 4 mg m^{-3} for the entire third phase of the upwelling event (Figure 7), and these concentrations

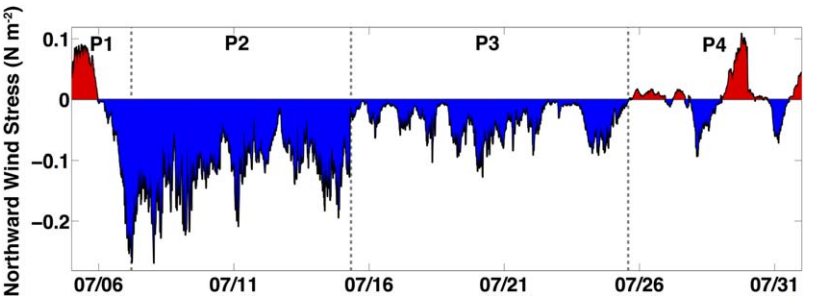

Figure 4. Northward wind stress (N m^{-2}) at the NDBC buoy 46050 (Figure 1) spanning the July 2008 upwelling event (Figure 2). Negative values indicate southward wind stress that drives offshore Ekman transport of the surface layer and coastal upwelling along the north-south oriented OR coast. Vertical dashed lines demarcate the phases of the upwelling event; where phase 1 (P1) is the transition from northward to peak southward wind stress (-0.27 N m^{-2}), phase 2 (P2) is the period of largely sustained southward wind stress < -0.05 N m^{-2}, phase 3 (P3) is the period of weaker southward wind stress, and phase 4 (P4) is the span of reversals in wind stress that proceeded the subsequent upwelling event that began 1 August (Figure 3).

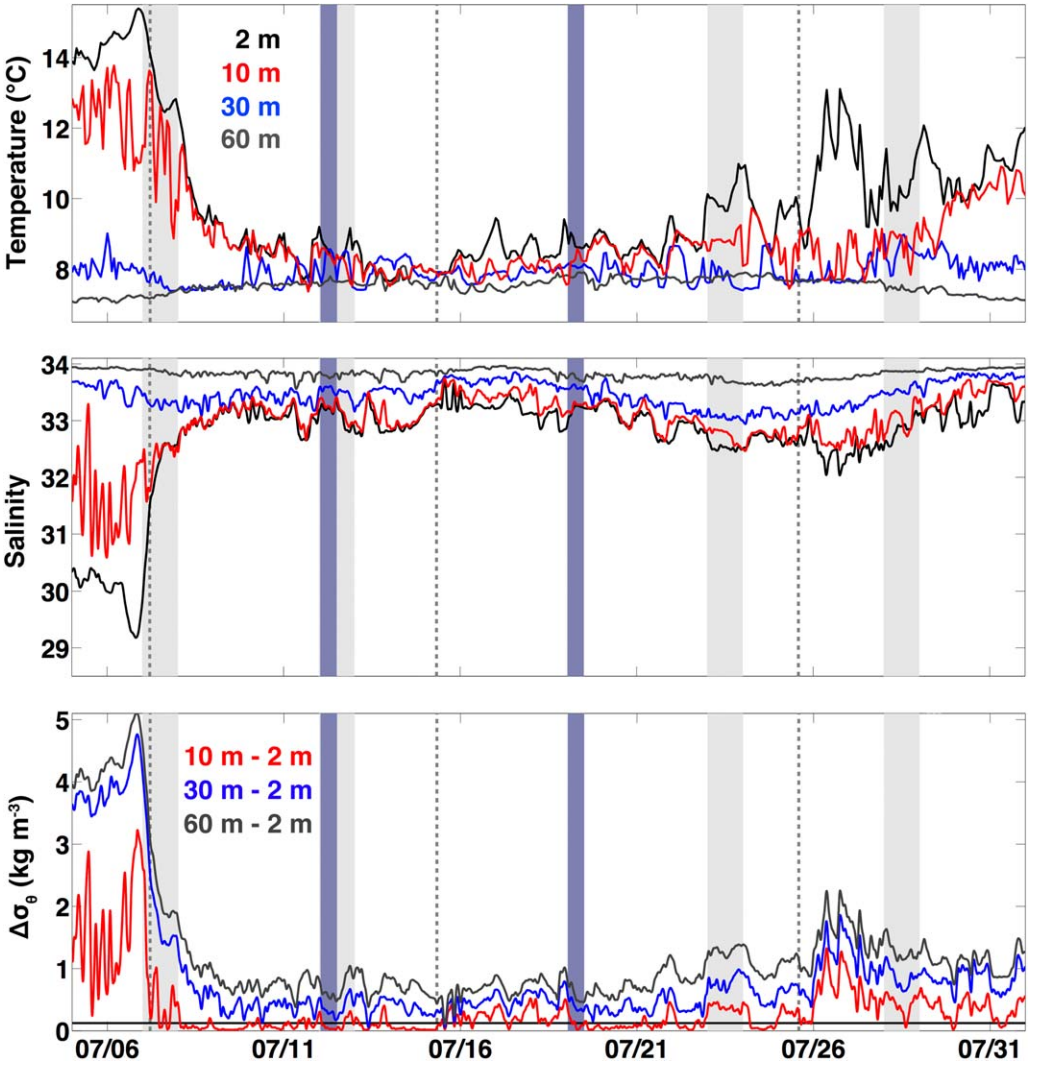

Figure 5. (top) Temperature (°C), (middle) salinity, and (bottom) potential density anomaly differences ($\Delta\sigma\theta$; kg m^{-3}) from the NH10 buoy site (Figure 1). Records are from 5 July to 3 August 2008. Depths where temperature and salinity data were recorded are indicated by color and the legend in the top plot. Corresponding $\Delta\sigma\theta$ at those depths, relative to $\sigma\theta$ at 2 m, are also indicated by color and the legend in the bottom plot. The horizontal black bar at $\Delta\sigma\theta = 0.125$ kg m^{-3} is a criterion for the depth of the mixed layer. Vertical dashed lines demarcate the phases following Figure 4. Vertical gray bars represent days when clear skies permitted the retrieval of MODIS SST and chlorophyll data. Vertical blue bars are days the NOAA Ship McArthur II passed by the NH10 buoy.

were also seen in the data collected by the NOAA ship *McArthur II* along the NH Line on its northward transit (Figure 9). The ΔO_2 and pCO_2 records from NH10 had trajectories that indicated a growing response from the phytoplankton community to the upwelling forcing, as both moved toward equilibrium with the atmosphere during phase 3 of the event (Figure 7). The concurrent adjustment of both gases, one of which being buffered by the marine carbon system, occurred without a coincident change in phytoplankton biomass (i.e., chlorophyll). The 20 day July upwelling event (Figure 3) ended when wind stress reversed on 25 July (Figure 4).

3.4. Phase 4: Wind Stress Reversals Preceding Next Upwelling Event

We consider phase 4 important because during this time the biogeochemistry of the coastal ocean continued to respond to the upwelling forcing prior to the start of the next upwelling event. From 25 July to 1 August, there were large, short-lived excursions in all parameters that were related to reversals in the wind stress and advection of water masses with distinct temperature and salinity characteristics, some of which are indicative of warmed upwelled water (Figure 5). Large changes in ΔO_2 and pCO_2 accompanied these changes in the water source. A warm, low-salinity surface layer moved past NH10 that initially drove an

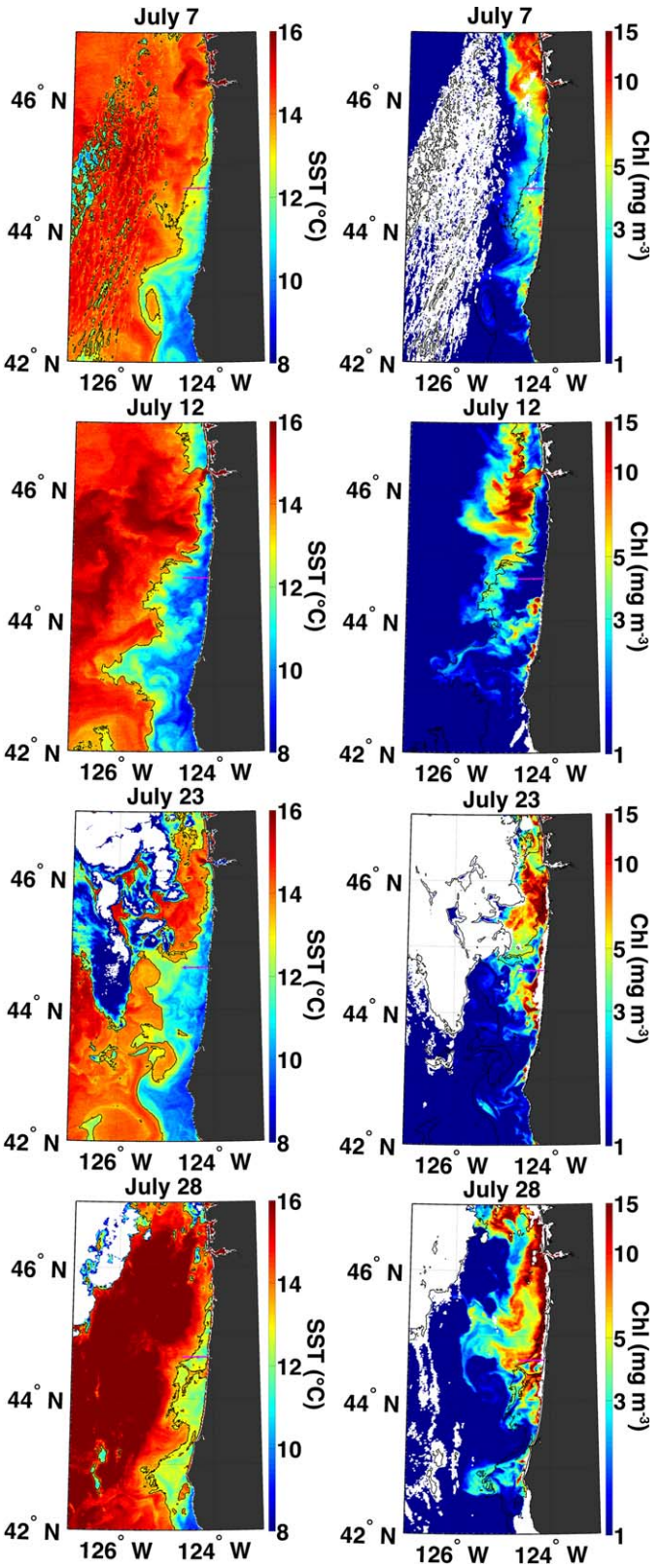

Figure 6. (left) MODIS Level 2 SST (°C) and (right) chlorophyll (mg m^{-3}) from individual passes on clear days spanning the July 2008 upwelling event. The black contours mark the 13.2°C SST contour, defined here as the position of the SST front between warm offshore water and cold recently upwelled water near shore (Figure 2). The magenta east-west horizontal bar is the NH Line extending from shore to the shelf break, and represents the shelf width west of Newport, OR. The dot near the center of this line is the OSU NH10 buoy position (Figure 1). Chlorophyll data are plotted in log scale. The offshore cool SSTs, most evident on 23 July, are cloud-contaminated data.

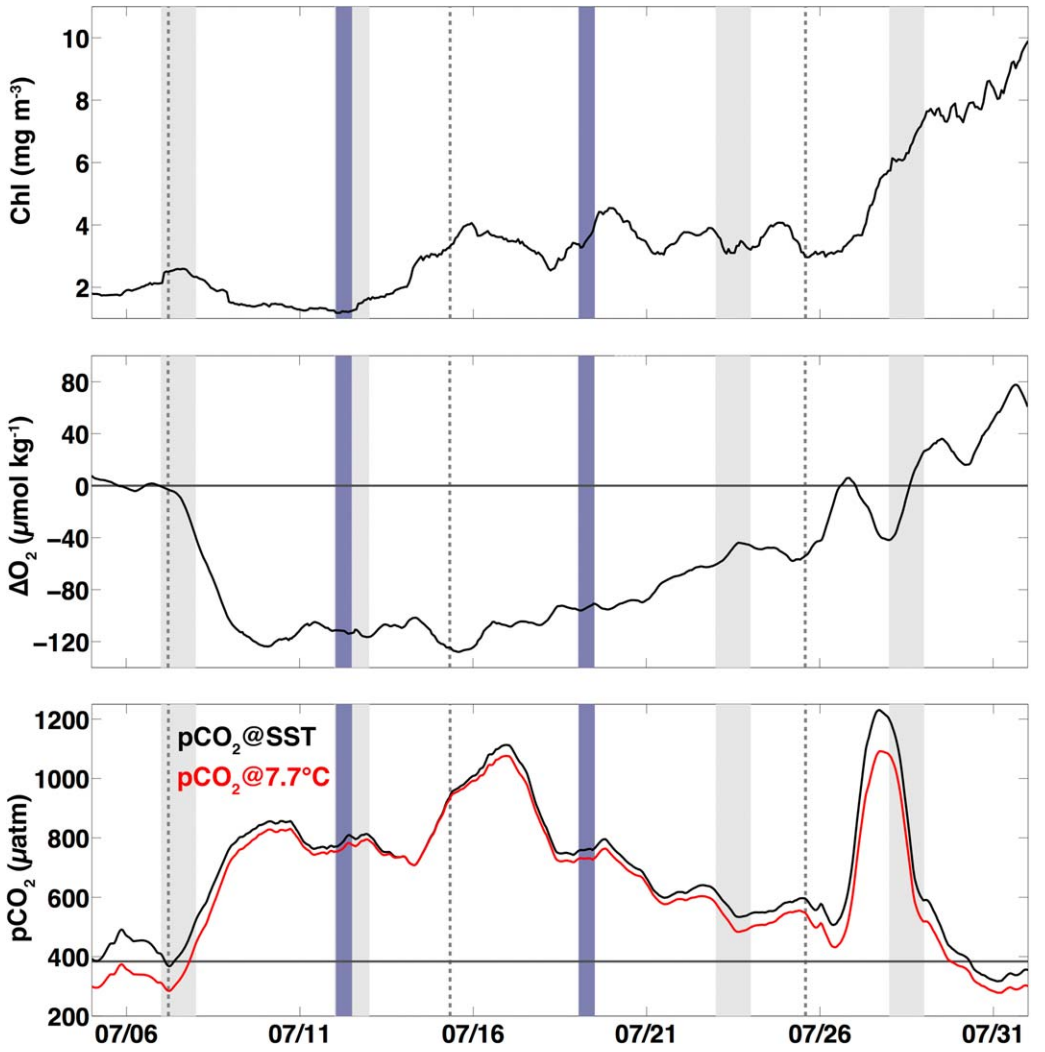

Figure 7. NH10 buoy surface data from 5 July to 1 August 2008: (top) chlorophyll (mg m^{-3}), (middle) ΔO2 (μmol kg^{-1}), and (bottom) pCO2 (μatm) at SST (black) and referenced to the minimum SST that occurred on 11 July (7.7°C; red line). Horizontal lines in the middle and bottom plots are saturation values for ΔO2 and pCO2, respectively. Vertical dashed lines demarcate the phases following Figure 4. Vertical gray bars were clear sky days when MODIS data were retrieved, and vertical blue bars are days the NOAA Ship McArthur II passed by the NH10 buoy.

increase in ΔO_2 and a decrease in pCO_2 over the course of a day (Figure 7). Another cooler and saltier surface layer then followed for a day with ΔO_2 near -40 μmol kg^{-1} and $pCO_{2(SST)}$ up to 1200 μatm (Figure 7). $pCO_{2(7.7°C)}$ was ∼150 μatm lower than $pCO_{2(SST)}$ during this brief episode, indicating that some of the observed pCO_2 increase was due to warming, but that most of the signal must have been from an increase in DIC that coincided with the ephemeral transition in the wind stress (Figure 7). This ephemeral event is difficult to diagnose with the buoy data alone, but highlights the rapidly changing conditions seen at the mooring site following this prolonged upwelling event as the water column is restructuring. In this Eulerian sense, variability in surface-water pCO_2 at the mooring is greatest during the transition period from upwelling to relaxation, and single point measurements during this time would be hugely misleading.

Between 28 July and 1 August, SSS at the mooring was near 33.5, equivalent to that observed previously in upwelled water, indicating that the water mass present at the mooring site at that time was aged upwelled water that had been at the surface long enough for SST to warm by ∼4°C (Figure 5). Phytoplankton biomass (i.e., chlorophyll) in this water had increased by five-fold from the values observed during the second phase of the upwelling event (Figure 7). MODIS chlorophyll data revealed that this increase at NH10 could be attributed to a large phytoplankton bloom that now spanned much of the shelf (Figure 6), and the SST front had regressed toward the coastline. The water mass present at the mooring site not only contained high

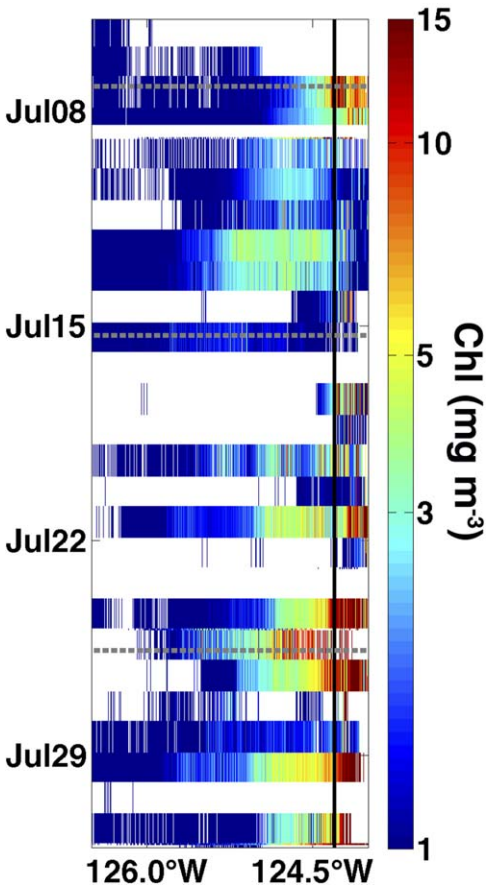

Figure 8. Time versus longitude Hovmuller section of MODIS Level 2 chlorophyll (mg m^{-3}) data from the on-offshore box shown in Figure 1. Chlorophyll data are in log scale and the black vertical line is the longitude of the OSU NH10 buoy. Gray dashed horizontal lines delineate the phases of the July 2008 upwelling event (Figure 4).

phytoplankton biomass (i.e., chlorophyll), but also the biogeochemical signatures of high rates of primary production. The large phytoplankton bloom drove high positive ΔO_2, and pCO_2 levels well below saturation with respect to the atmosphere (Figure 7), ending a 23 day period of sustained CO_2 outgassing. The end of outgassing at NH10 lagged the first reversal in wind stress by 5 days (Figures 4 and 7).

4. Discussion

The observations presented span the strongest and longest period of sustained upwelling on the OR coast in 2008 (Figure 3), and this event caused the prolonged exposure of high-pCO_2 water to the atmosphere on the Oregon shelf (Figures 5 and 7). The combination of high wind speeds and persistent oversaturation of surface-water pCO_2 generated large fluxes that had a significant impact on the annual sea-air CO_2 exchange estimated for this region [*Evans et al.*, 2011]. Here we aim to elucidate the apparent lack of a phytoplankton response shortly following the initiation of this upwelling event that should have drawn down the elevated pCO_2, thereby driving the shelf toward a net sink for CO_2 as described by *Hales et al.* [2005b]. Had the water experienced full biological response over the 9 day period of sustained strong southward wind stresses described above, chlorophyll concentrations could have reached levels above 35 mg m^{-3} assuming no loss terms, complete nitrate utilization, and a conservative doubling time of 0.5 day^{-1} with the initial chlorophyll concentration of 2 mg m^{-3} seen at the NH10 buoy site (Figure 5). This net phytoplankton growth and nitrate uptake would have resulted in a ΔO_2 increase by 350 mmol m^{-3}, and a pCO_2 decrease to values below 200 μatm. None of these were observed, however, as there was no evidence of increased chlorophyll at the mooring site or downstream of the region of active upwelling through the first two phases of this event. From our satellite, ship and mooring perspectives, it appeared as if the coastal ocean off Oregon was not conducive to a strong phytoplankton response from the large pulse of upwelled nutrients until more relaxed conditions were reached during phase 3. *Wilkerson et al.* [2006] report that the optimal window for a phytoplankton bloom to accumulate is 3–7 days following an upwelling pulse based on results collected during the Coastal Ocean Processes: Wind Events and Shelf Transport (CoOP WEST) study. From our results, this optimal window didn't appear to initiate until the start of phase 3 of the July 2008 upwelling event.

We believe a number of limiting factors can immediately be excluded as possible causes for retarding the development of a phytoplankton bloom in response to the 2008 upwelling event. All previous data have shown tight coupling between high pCO_2 and low O_2, as did our validations samples here, so macronutrient limitation cannot be implicated. Iron limitation can not be invoked here because OR shelf waters are high in iron, and iron stress has never been demonstrated [*Chase et al.*, 2005, 2007]. High ammonium concentrations can inhibit nitrate uptake in upwelling regions [*Kokkinakis and Wheeler*, 1987], however the values observed during our cruise were at most 0.8 μM (W. Peterson, unpublished data, 2008) and not high enough to cause a long delay in phytoplankton growth (P. Wheeler, personal communication, 2011). Seed stock can not be an issue here because incubation studies using water collected below the mixed layer

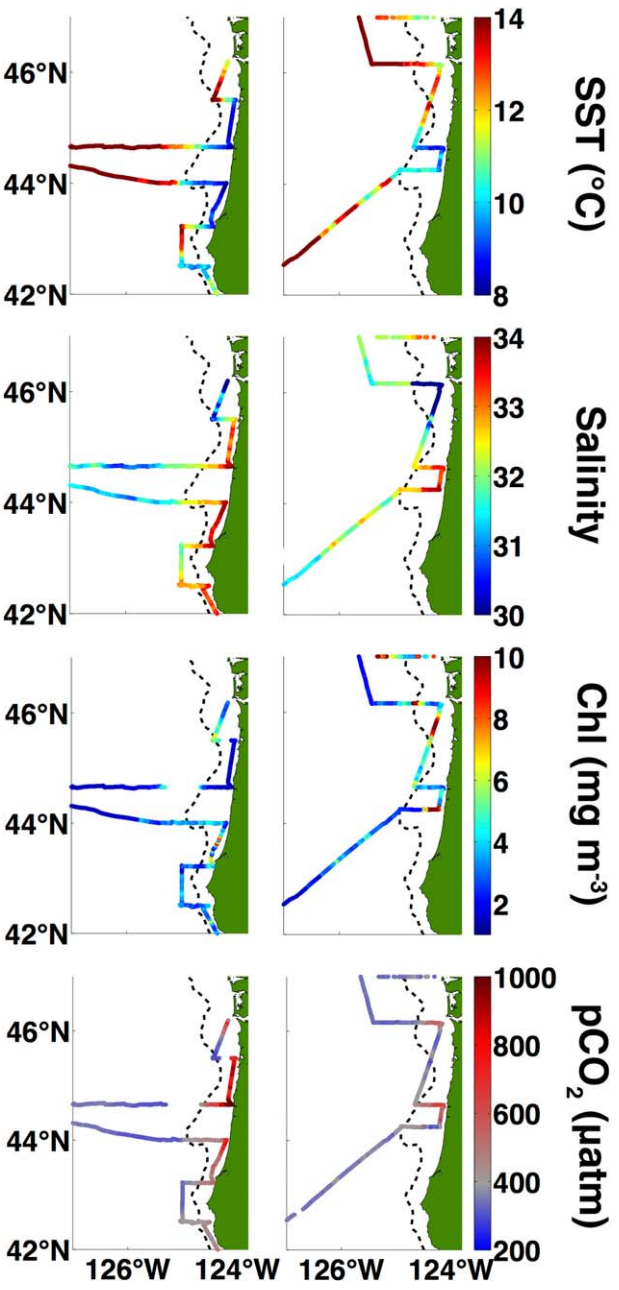

Figure 9. (left) SST (°C), salinity, chlorophyll (mg m^{-3}) and pCO2 (µatm) from the southbound portion of the cruise aboard the NOAA Ship McArthur II (12–17 July 2008). (right) Same as the left but for the northbound portion of the cruise (17–21 July 2008).

(∼28 to 70 m) and from the benthic boundary layer have developed blooms on the order of days [*Wetz and Wheeler*, 2003; *Wetz et al*., 2004]. Similarly, light limitation likely is not a factor because growth was observed to occur at 40–50% of the surface irradiance in winter [*Wetz et al*., 2004]. Also, based on estimating the mixed layer depth by a density difference of 0.125 kg m^{-3} from a 2 m reference level, the mixed layer was consistently shallower than 30 m (Figure 5). For there to be a deleterious effect on phytoplankton growth from a deep mixed layer, we should anticipate a large decoupling between mixed layer depth and euphotic zone depth, and that was likely not encountered during July 2008.

One process that most likely explains the delay of a large bloom is the short exposure time of upwelled water to the surface. While the intense upwelling persisted for 9 days, the water as it passed the mooring had probably never been at the surface for a comparable amount of time. Cross-shelf transport affects the exposure time of freshly upwelled water at the surface, in that the slower the transport for a given distance between outcropping and subduction points, the longer upwelled water will be in contact with the atmosphere over the shelf before encountering and subducting underneath lighter offshore waters [*Austin and Barth*, 2002; *Flament et al*., 1985; *Fortier et al*., 2008]. Estimates of the exposure time of freshly upwelled water at the mooring site can be made from both the physical and chemical data. The average PFEL 6 hourly upwelling index over the 7–15 July period of strong upwelling was 107 m^3/s/100 m of coastline. Assuming a surface mixed layer of 20 m and that upwelled water first outcrops at the beach in Newport, OR (∼20 km from the mooring site), this equates to a cross-shelf velocity of nearly 5 km d^{-1} and an exposure time of 4 days for the water prior to reaching the mooring location. Exposure time can also be estimated using the oxygen data, and since dissolved O_2 is not a buffered gas, unlike CO_2, its response to gas exchange is rapid. The period of persistent strongly undersaturated ΔO_2 between 10 and 15 July in the face of swift gas exchange implies very short exposure times. Given a gas transfer velocity for O_2 of 6 m d^{-1} based on mean wind speeds for this phase of the upwelling event and the gas transfer formulation of *Ho et al*. [2011], and a 20 m mixed layer, the response time for O_2 to reach equilibration with the atmosphere should be ∼3 days; however we saw strongly undersaturated O_2 during this interval, suggesting a much shorter surface exposure time. Based on these physical and chemical estimates, the exposure time of upwelled water at NH10 during the period of

strong upwelling was at most 4 days, but likely shorter, given the assumption of a maximal cross-shelf distance between the mooring and the hypothetical locus of upwelling.

During upwelling conditions, inner to midshelf surface water is generally moving alongshore and offshore [*Barth et al*., 2005; *Kosro*, 2005] such that the possibility exists for a phytoplankton bloom downstream of the upwelling center near Newport OR. However, no downstream phytoplankton bloom was observed in MODIS data (Figure 6) or from the ship (Figure 8), which supports the idea that upwelled water on the central Oregon shelf was exposed to the atmosphere for only a short period relative to the time needed for a phytoplankton bloom to occur during the July 2008 upwelling event. Recently upwelled water was not at the surface long enough for a large phytoplankton response to occur so as to draw pCO_2 down to below atmospheric levels and prevent the large effluxes that were reported by *Evans et al*. [2011].

Subduction of recently upwelled water must be occurring in order for no large phytoplankton bloom to develop on the time scale expected ($\sim$5 days) in the face of a shallow mixed layer ($<$30 m), typically strong summer solar irradiances and presumably ample nutrients following the initiation of the July 2008 upwelling event. Only within a small region of Heceta Bank did satellite data show any indication of blooming phytoplankton (Figure 6) during the period of strong upwelling (Figure 4). We hypothesize that the subduction of cold, freshly upwelled surface water below warmer offshore surface water at convergent SST fronts may be responsible for the decoupling between upwelling and productivity that resulted in persistent CO_2 efflux to the atmosphere. Evidence of subduction in coastal upwelling settings exists, with strong vertical transport having been observed to inject coastal chlorophyll and biogenic particulate carbon below the euphotic zone in offshore waters [*Barth et al*., 2002; *Flament et al*., 1985; *Kadko et al*., 1991]. However, these studies do not agree on the exact physical mechanism driving this process. *Flament et al*. [1985] suggested the mechanism was driven by the convergence of heavier coastal water with lighter offshore water, which may relate to a secondary circulation pattern within the more general concept of coastal upwelling [*Allen et al*., 1995; *Mooers et al*., 1976] that can result in vertical transports on the order of 9 m d^{-1} [*Flament et al*., 1985]. *Kadko et al*. [1991] did not suggest a mechanism for the deep chlorophyll feature they observed offshore, however they proposed vertical velocities of 27 m d^{-1} based on the ^{222}Rn deficit in subducted water. *Barth et al*. [2002] suggested that offshore deep chlorophyll features are caused by the conservation of potential vorticity along the meandering path of the California Current jet [*Barth et al*., 2005]. As a coastal water mass is moved offshore, the water column height increases, and the water mass is forced downward along sloping isopycnals.

Serendipitously, a Slocum glider occupation of the NH Line during the July 2008 upwelling event captured a deep chlorophyll feature that originated at the surface near shore and extended to near 70 m offshore of the NH10 buoy position (Figure 10). We can estimate the depth of limiting photon flux using the compensation light intensity reported by *Wetz et al*. [2004] and MODIS Level 2 photosynthetically active radiation (PAR) and diffuse attenuation coefficient at 490 nm (k_{490}) data. The depth of limiting photon flux is defined as: $Z_{LPF} = \ln(0.75/PAR)/k_{490}$, where 0.75 is the compensation light intensity (mol quanta m^{-2} d^{-1}). Figure 11 shows Z_{LPF} for 12 and 23 July, clear-sky dates bracketing the glider transect. Even during the day of more intense upwelling and lowest surface chlorophyll concentrations, the Z_{LPF} was broadly 60 m near shore to 30 m over the outer shelf. These depths shoaled by 23 July, indicated that the chlorophyll feature observed by the glider was not produced locally, but injected from the surface layer above the depth of the Z_{LPF}. We note that this chlorophyll feature appears to originate at the surface inshore of NH10, and is spatially distinct for the large-scale SST front that separates recently upwelled shelf water from warm offshore waters [*Austin and Barth*, 2002; *Flament et al*., 1985; *Fortier et al*., 2008]. This suggests that there may be multiple loci of upwelling, whereby typical coastal upwelling occurs in concert with wind-stress curl induced upwelling [*Dever et al*., 2006]. With multiple loci of upwelling, it is then also possible that there are multiple regions of subduction, and the SST gradient we defined above as the region of subduction is one of many in this dynamic coastal setting. Only when upwelling/downwelling conditions settle down can there be an accumulation of phytoplankton biomass resulting in drawn down surface-water pCO_2. This is consistent with the results of the CoOP West study that report most optimal conditions for phytoplankton accumulation during periods of lower upwelling index and longer sustained relaxation [*Wilkerson et al*., 2006]. There is not a consensus yet as to the mechanism that causes subducting features in the coastal ocean, however there is no disagreement that deep features of coastal origin do exist. Subduction processes were likely responsible for removing freshly upwelled surface water during the July 2008 upwelling event, preventing the

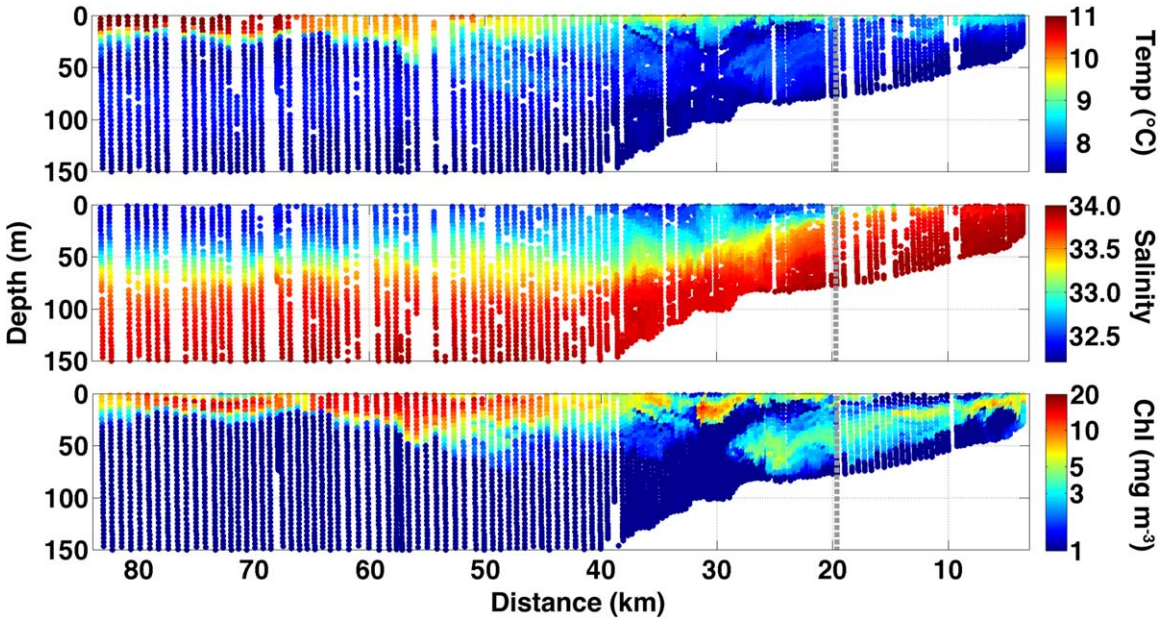

Figure 10. Depth (m) versus distance from shore (km) sections of (top) temperature (°C), (middle) salinity, and (bottom) chlorophyll (mg m^{-3}) data collected by an OSU Slocum glider between 17 and 21 July 2008 along a transect of the NH Line during Phase 3 of the upwelling event. The gray dashed vertical line marks the position of the NH10 buoy (Figure 1). Chlorophyll data are on a log scale.

development of a phytoplankton bloom and allowing the persistence of high-pCO_2 conditions over the central Oregon shelf. This of course has consequences for the DIC and nutrient status of ocean interior waters, and the subsequent biological response, when they outcrop once again at the ocean surface.

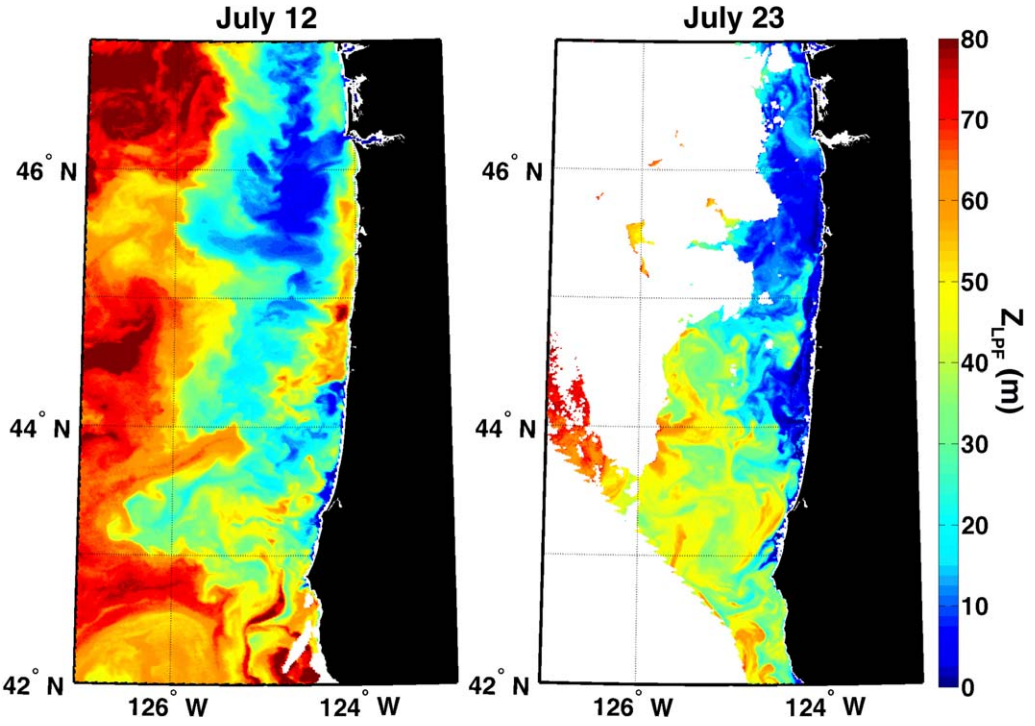

Figure 11. Depth of limiting photon flux (ZLFP; m) for (left) 12 July and (right) 23 July. Depth of limiting photon flux was calculated by altering the equation for estimating the depth of the euphotic zone, Zeu = ln(0.01)/k490, to ZLPF = ln(0.75/PAR)/k490, where 0.75 is the compensation light intensity (mol quanta m^{-2} d^{-1}) reported by *Wetz et al.* [2004], PAR is MODIS Level 2 photosynthetically active radiation (mol quanta m^{-2} d^{-1}) and k490 is the diffuse attenuation coefficient at 490 nm.

The July 2008 upwelling event was remarkable in that it caused high-pCO_2 water to persist at the surface for an extended period of time due to the slow phytoplankton response in comparison to the short exposure time for recently upwelled water. Additional lines of evidence that short exposure time of upwelled water caused a negligible phytoplankton response are the changes in chlorophyll, ΔO_2 and pCO_2 at NH10 that coincided with the decrease in southward wind stress. During phase 3 of the upwelling event, the average daily PFEL upwelling index was 54 m^3/s/100 m of coastline. Assuming, again, a 20 m mixed layer and that upwelled water outcrops adjacent to the coast, this implies a longer exposure time of 9 days that permitted a phytoplankton response from the upwelling event. The slight increase in chlorophyll, steady increase in ΔO_2 and the decrease in pCO_2 during this period are all photosynthetic trends and evidence of an initiating phytoplankton response to the upwelling-supplied nutrients enabled by a longer exposure time of upwelled water. During phase 2 of the upwelling event, short exposure time of upwelled water was driven by strong southward wind stresses, rapid cross-shelf transport and subsequent subduction at convergent SST fronts. There is mounting evidence of increased upwelling intensity and persistence over the 20th century [*Bakun*, 1990; *García-Reyes and Largier*, 2010, 2012; *McGregor et al*., 2007; *Merryfield et al*., 2009; *Sydeman et al*., 2014; *Toggweiler and Russell*, 2008], with upwelling intensity predicted to increase under climate change scenarios [*Snyder et al*., 2003; *Sydeman et al*., 2014; *Toggweiler and Russell*, 2008]. In addition, the surface warming of open ocean waters predicted by climate change scenarios [*Levitus et al*., 2000] will result in a stronger contrast between offshore waters and upwelled water on the shelf, and therefore stronger convergent SST fronts. Thus, as upwelling intensity increases and the surface waters of the offshore North Pacific warm, the unchecked outgassing observed during July 2008 will become more prevalent.

Episodes of prolonged outgassing have significant implications for carbon cycling in these coastal waters in a changing climate. First, *Evans et al*. [2011] showed that these events have a significant impact on the net annual sea-air CO_2 exchange for the region. System changes leading to dominance of these conditions would shift this region from a significant net annual sink for atmospheric CO_2 to a net annual source. Second, *Hales et al*. [2006] suggested that the absence of relaxation events could be linked to on-shelf retention of particulate organic carbon produced by shelf phytoplankton. Under the conditions seen during the July 2008 upwelling event, the lack of a strong phytoplankton response would imply low vertical particulate organic carbon export to shelf bottom waters. The local respiration signal in already low-O_2 upwelling source waters should therefor be minimized due to this reduced input and not add to on-shelf hypoxia, perhaps slowing the apparent trend of increasing hypoxia reported by *Chan et al*. [2008]. Finally, low aragonite and calcite saturation states characterize high-pCO_2 upwelled water in this region [*Feely et al*., 2008; *Harris et al*., 2013]. During this event in July 2008, oyster seed production collapsed at the Whiskey Creek Hatchery in Netarts Bay, OR [*Barton et al*., 2012; *Scigliano*, 2011]. The failure in production was caused by the introduction of corrosive upwelled waters into the hatchery during the July event [*Barton et al*., 2012; *Kerr*, 2010]. If these events become more prevalent in the future, the consequences for coastal marine life due to increased exposure to corrosive waters are clearly serious and will have cascading economic effects.

5. Conclusions

The data presented are from a prolonged and intense upwelling event in July 2008 that had a large impact on the annual sea-air CO_2 flux for the central Oregon midshelf. Exposure time of upwelled water to the atmosphere was rapid relative to phytoplankton response times, and was followed by subduction below low-density offshore waters at convergent SST fronts prior to bloom formation. Once upwelling weakened, exposure time lengthened, and a phytoplankton response to the upwelling-supplied nutrients was observed. These observations show that the surface exposure time of upwelled water is critical for a phytoplankton response and CO_2 drawdown, with consequences for the overall sink/source nature of the shelf, the chemical composition of the offshore subducted waters and the exposure of coastal animals to hypoxic and corrosive waters.

Acknowledgments

We thank Murray Levine, Craig Risien and Walt Waldorf for the NH-10 buoy platform and data, which is funded by the National Science Foundation through the cooperative agreement OCE-0424602 known as CMOP (Coastal Margin Observation and Prediction) and by NOAA through NANOOS (Northwest Association of Networked Ocean Observing Systems), the Pacific Northwest Regional Association of the U.S. Integrated Ocean Observing System (IOOS). We also thank Patricia Wheeler for her valuable input that improved this manuscript. We also thank Bill Peterson for allowing our participation in the July 2008 cruise, and for sharing data with us from that cruise. We thank the officers and crew of the NOAA Ship *McArthur II*. Internet links to the various datasets used in this manuscript are provided in the methods section, and readers may find the pCO_2 data in the Coastal Carbon Data archive at the Carbon Dioxide Information and Analysis Center (http://cdiac.ornl.gov/oceans/coastal_carbon_data.html). The glider data collection and analyses were supported by NSF OCE-0527168 and OCE-0961999 to JAB and RKS. This work was supported by NSF Chemical Oceanography award OCE-0752576.

References

Allen, J. S., P. A. Newberger, and J. Federiuk (1995), Upwelling circulation on the Oregon Continental Shelf. Part I: Response to idealized forcing, *J. Phys. Oceanogr.*, *25*, 1843–1866.

Austin, J. A., and J. A. Barth (2002), Variation in the position of the upwelling front on the Oregon shelf, *J. Geophys. Res.*, *107*(C11), 3180, doi: 10.1029/2001JC000858.

Bakun, A. (1990), Global climate change and intensification of coastal ocean upwelling, *Science*, *247*, 198–201.
Barth, J. A., T. J. Cowles, P. M. Kosro, R. K. Shearman, A. Huyer, and R. L. Smith (2002), Injection of carbon from the shelf to offshore beneath the euphotic zone in the California Current, *J. Geophys. Res.*, *107*(C6), 3057, doi:10.1029/2001JC000956.
Barth, J. A., S. D. Pierce, and T. Cowles (2005), Mesoscale structure and its seasonal evolution in the northern California Current System, *Deep Sea Res., Part II*, *52*, 5–28.
Barth, J. A., B. A. Menge, J. Lubchenco, F. Chan, J. M. Bane, A. R. Kirincich, M. A. McManus, K. J. Nielsen, S. D. Pierce, and L. Washburn (2007), Delayed upwelling alters nearshore coastal ocean ecosystems in the northern California current, *Proc. Natl. Acad. Sci. U. S. A.*, *104*(10), 3719–3724.
Barton, A., B. Hales, G. Waldbusser, C. Langdon, and R. A. Feely (2012), The Pacific oyster, *Crassostrea gigas*, shows negative correlation to naturally elevated carbon dioxide levels: Implications for near-term ocean acidification effects, *Limnol. Oceanogr. Methods*, *57*(3), 698–710.
Borges, A. V. (2005), Do we have enough pieces of the jigsaw to integrate CO_2 fluxes in the coastal ocean?, *Estuaries*, *28*(1), 3–27.
Borges, A. V., B. Delille, and M. Frankignoulle (2005), Budgeting sinks and sources of CO_2 in the coastal ocean: Diversity of ecosystems counts, *Geophys. Res. Lett.*, *32*, L14601, doi:10.1029/2005GL023053.
Cai, W.-J., M. Dai, and Y. Wang (2006), Air-sea exchange of carbon dioxide in ocean margins: A province-based synthesis, *Geophys. Res. Lett.*, *33*, L12603, doi:10.1029/2006GL026219.
Chan, F., J. A. Barth, J. Lubchenco, A. Kirincich, H. Weeks, W. T. Peterson, and B. A. Menge (2008), Emergence of anoxia in the California Current Large Marine Ecosystem, *Science*, *319*(5865), 280, doi:10.1126/science.1149016.
Chase, Z., B. Hales, T. Cowles, R. Schwartz, and A. van Geen (2005), Distribution and variability of iron input to Oregon coastal waters during the upwelling season, *J. Geophys. Res.*, *110*, C10S12, doi:10.1029/2004JC002590.
Chase, Z., P. G. Strutton, and B. Hales (2007), Iron links river runoff and shelf width to phytoplankton biomass along the U.S. West Coast, *Geophys. Res. Lett.*, *34*, L04607, doi:10.1029/2006GL028069.
Chavez, F. P., T. Takahashi, W.-J. Cai, G. E. Friederich, B. Hales, R. Wanninkhof, and R. A. Feely (2007), Coastal oceans, in *The First State of the Carbon Cycle Report (SOCCR): The North American Carbon Budget and Implications for the Global Carbon Cycle*, edited by A. W. King et al., pp. 157–166, U.S. Clim. Change Sci. Program, Washington, D. C.
Dai, M., Z. Cao, X. Guo, W. Zhai, Z. Liu, Z. Yin, Y. Xu, J. Gan, J. Hu, and C. Du (2013), Why are some marginal seas sources of atmospheric CO_2?, *Geophys. Res. Lett.*, *40*, 2154–2158, doi:10.1002/grl.50390.
DeGrandpre, M. D., T. R. Hammar, S. P. Smith, and F. L. Sayles (1995), In situ measurements of seawater pCO_2, *Limnol. Oceanogr.*, *40*(5), 969–975.
DeGrandpre, M. D., T. R. Hammar, D. W. R. Wallace, and C. D. Wirick (1997), Simultaneous mooring-based measurements of seawater CO_2 and O_2 off Cape Hatteras, North Carolina, *Limnol. Oceanogr.*, *42*(1), 21–28.
DeGrandpre, M. D., G. J. Olbu, C. M. Beatty, and T. R. Hammar (2002), Air-sea CO_2 fluxes on the US Middle Atlantic Bight, *Deep Sea Res., Part II*, *49*, 4355–4367.
Dever, E. P., C. E. Dorman, and J. L. Largier (2006), Surface boundary-layer variability off Northern California, USA, during upwelling, *Deep Sea Res., Part II*, *53*(25-26), 2887–2905, doi:10.1016/j.dsr2.2006.09.001.
Dickson, A. G., C. L. Sabine, and J. R. Christian (Eds.) (2007), PICES Special Publication 3, IOCCP Report No. 8, *Guide to Best Practices for Ocean CO2 Measurements*, 191 pp., North Pac. Mar. Sci. Organ., Sidney, British Columbia.
Dugdale, R. C., F. P. Wilkerson, V. E. Hogue, and A. Marchi (2006), Nutrient controls on new production in the Bodega Bay, California, coastal upwelling plume, *Deep Sea Res., Part II*, *53*(25-26), 3049–3062.
Evans, W., B. Hales, and P. G. Strutton (2011), The seasonal cycle of surface ocean pCO_2 on the Oregon shelf, *J. Geophys. Res.*, *116*, C05012, doi:10.1029/2010JC006625.
Evans, W., B. Hales, P. G. Strutton, and D. Ianson (2012), Sea-air CO_2 fluxes in the western Canadian coastal ocean, *Prog. Oceanogr.*, *101*, 78–91, doi:10.1016/j.pocean.2012.1001.1003.
Evans, W., B. Hales, and P. G. Strutton (2013), pCO_2 distributions and air-water CO_2 fluxes in the Columbia River estuary, *Estuarine Coastal Shelf Sci.*, *117*, 260–272. doi:10.1016/j.ecss.2012.1012.1003.
Feely, R. A., C. L. Sabine, M. Hernandez-Ayon, D. Ianson, and B. Hales (2008), Evidence for upwelling of corrosive "acidified" water onto the continental shelf, *Science*, *320*(5882), 1490–1492.
Flament, P., L. Armi, and L. Washburn (1985), The evolving structure of an upwelling filament, *J. Geophys. Res.*, *90*(C6), 11,765–11,778.
Fortier, R., R. K. Shearman, J. A. Barth, A. Erofeev, L. Rubiano-Gomez, and J. G. Brodersen (2008), Autonomous glider observations of subducting tongues of warm, high-chlorophyll water on the Oregon Shelf, paper presented at 2008 AGU Fall Meeting, AGU, San Francisco, Calif.
Friederich, G. E., P. M. Walz, M. G. Burczynski, and F. P. Chavez (2002), Inorganic carbon in the central California upwelling system during the 1997–1999 El Niño-La Niña event, *Prog. Oceanogr.*, *54*, 185–203.
García, H. E., and L. I. Gordon (1992), Oxygen solubility in seawater: Better fitting equations, *Limnol. Oceanogr.*, *37*(6), 1301–1312.
García-Reyes, M., and J. Largier (2010), Observations of increased wind-driven coastal upwelling off central California, *J. Geophys. Res.*, *115*, C04011, doi:10.1029/2009JC005576.
García-Reyes, M., and J. L. Largier (2012), Seasonality of coastal upwelling off central and northern California: New insights, including temporal and spatial variability, *J. Geophys. Res.*, *117*, C03028, doi:10.1029/2011JC007629.
Hales, B., D. Chipman, and T. Takahashi (2004), High-frequency measurements of partial pressure and total concentration of carbon dioxide in seawater using microporous hydrophobic membrane contactors, *Limnol. Oceanogr. Methods*, *2*, 356–364.
Hales, B., L. Karp-Boss, A. Perlin, and P. A. Wheeler (2006), Oxygen production and carbon sequestration in an upwelling coastal margin, *Global Biogeochem. Cycles*, *20*, GB3001, doi:10.1029/2005GB002517.
Hales, B., J. N. Moum, P. Covert, and A. Perlin (2005a), Irreversible nitrate fluxes due to turbulent mixing in a coastal upwelling system, *J. Geophys. Res.*, *110*, C10S11, doi:10.1029/2004JC002685.
Hales, B., T. Takahashi, and L. Bandstra (2005b), Atmospheric CO_2 uptake by a coastal upwelling system, *Global Biogeochem. Cycles*, *19*, GB1009, doi:10.1029/2004GB002295.
Hales, B., W.-J. Cai, B. G. Mitchell, C. L. Sabine, and O. Schofield (2008), *North American Continental Margins: A Synthesis and Planning Workshop*, 110 pp., U.S. Carbon Cycle Sci. Program, Washington, D. C.
Hales, B., P. G. Strutton, M. Saraceno, R. Letelier, T. Takahashi, R. A. Feely, C. L. Sabine, and F. P. Chavez (2012), Satellite-based prediction of pCO_2 in coastal waters of the eastern North Pacific, *Prog. Oceanogr.*, *103*, 1–15.
Harris, K. E., M. D. Degrandpre, and B. Hales (2013), Aragonite saturation state dynamics in a coastal upwelling zone, *Geophys. Res. Lett.*, *40*, 2720–2725, doi:10.1002/grl.50460.

Hill, J. K., and P. A. Wheeler (2002), Organic carbon and nitrogen in the northern California current system: Comparison of offshore, river plume, and coastally upwelled waters, *Prog. Oceanogr.*, *53*, 369–387.

Ho, D. T., R. Wanninkhof, P. Schlosser, D. S. Ullman, D. Hebert, and K. F. Sullivan (2011), Toward a universal relationship between wind speed and gas exchange: Gas transfer velocities measured with $^3He/SF_6$ during the Southern Ocean Gas Exchange Experiment, *J. Geophys. Res.*, *116*, C00F04, doi:10.1029/2010JC006854.

Holm-Hansen, O. (1978), Chlorophyll a determination: Improvements in methodology, *Oikos*, *30*(3), 438–447.

Huyer, A., J. H. Fleischbein, J. Keister, P. M. Kosro, N. Perlin, R. L. Smith, and P. A. Wheeler (2005), Two coastal upwelling domains in the northern California Current system, *J. Mar. Res.*, *63*, 901–929.

Huyer, A., P. A. Wheeler, P. T. Strub, R. L. Smith, R. Letelier, and P. M. Kosro (2007), The Newport line off Oregon—Studies in the North East Pacific, *Progr. Oceanogr.*, *75*, 126–160.

Jiang, L.-Q., W.-J. Cai, R. Wanninkhof, Y. Wang, and H. Lüger (2008), Air-sea CO_2 fluxes on the U.S. South Atlantic Bight: Spatial and seasonal variability, *J. Geophys. Res.*, *113*, C07019, doi:10.1029/2007JC004366.

Kadko, D. C., L. Washburn, and B. Jones (1991), Evidence of subduction within cold filaments of the Northern California coastal transition zone, *J. Geophys. Res.*, *96*(C8), 14,909–14,926.

Kerr, R. A. (2010), Ocean acidification unprecedented, unsettling, *Science*, *328*, 1500–1501.

Kokkinakis, S. A., and P. A. Wheeler (1987), Nitrogen uptake and phytoplankton growth in coastal upwelling regions, *Limnol. Oceanogr.*, *32*(5), 1112–1123.

Kosro, P. M. (2005), On the spatial structure of coastal circulation off Newport, Oregon, during spring and summer 2001 in a region of varying shelf width, *J. Geophys. Res.*, *110*, C10S06, doi:10.1029/2004JC002769.

Laruelle, G. G., H. H. Dürr, C. P. Slomp, and A. V. Borges (2010), Evalution of sinks and sources of CO_2 in the global coastal ocean using a spatially-explicit typology of estuaries and continental shelves, *Geophys. Res. Lett.*, *37*, L15607, doi:10.1029/2010GL043691.

Levitus, S., J. I. Antonov, T. P. Boyer, and C. Stephens (2000), Warming of the World Ocean, *Science*, *287*, 2225–2229.

McGregor, H. V., M. Dima, and H. W. M. Fischer, S. (2007), Rapid 20th-century increase in coastal upwelling off Northwest Africa, *Science*, *315*(5812), 637–639.

Merryfield, W. J., B. Pal, and M. G. G. Foreman (2009), Projected future changes in surface marine winds off the west coast of Canada, *J. Geophys.Res.*, *114*, C06008, doi:10.1029/2008JC005123.

Mooers, C. N. K., C. A. Collins, and R. L. Smith (1976), The dynamic structure of the frontal zone in the coastal upwelling region off Oregon, *J. Phys. Oceanogr.*, *6*(1), 3–21.

Pierce, S., J. A. Barth, R. E. Thomas, and G. W. Fleischer (2006), Anomalously warm July 2005 in the northern California Current: Historical context and the significance of cumulative wind stress, *Geophys. Res. Lett.*, *33*, L22S04, doi:10.1029/2006GL027149.

Scigliano, E. (2011), The great oyster crash, in *OnEarth*, Nat. Resour. Defense Counc., N. Y. [Available at http://archive.onearth.org/article/oyster-crash-ocean-acidification.]

Snyder, M. A., L. C. Sloan, N. S. Diffenbaugh, and J. L. Bell (2003), Future climate change and upwelling in the California Current, *Geophys. Res. Lett.*, *30*(15), 1823, doi:10.1029/2003GL017647.

Sydeman, W. J., M. García-Reyes, D. S. Schoeman, R. R. Rykaczewski, S. A. Thompson, B. A. Black, and S. J. Bograd (2014), Climate change and wind intensification in coastal upwelling ecosystems, *Science*, *345*(6192), 77–80, doi:10.1126/science.1251635.

Takahashi, T., J. Olafsson, J. G. Goddard, D. W. Chipman, and S. C. Sutherland (1993), Seasonal variation of CO_2 and nutrients in the high-latitude surface oceans: A comparative study, *Global Biogeochem. Cycles*, *7*(4), 843–878; doi:10.1029/93GB02263.

Takahashi, T., et al. (2002), Global sea-air CO_2 flux based on climatological surface ocean pCO2, and seasonal biological and temperature effects, *Deep Sea Res., Part II*, *49*, 1601–1622.

Takahashi, T., et al. (2009), Climatological mean and decadal change in surface ocean pCO_2 and net sea-air CO_2 flux over the global oceans, *Deep Sea Res., Part II*, *56*, 554–577.

Toggweiler, J. R., and J. Russell (2008), Ocean Circulation in a warming climate, *Nature*, *451*, 286–288.

van Geen, A., R. K. Takesue, J. Goddard, T. Takahashi, J. A. Barth, and R. L. Smith (2000), Carbon and nutrient dynamics during coastal upwelling off Cape Blanco, Oregon, *Deep Sea Res., Part II*, *47*, 975–1002.

Wetz, M. S., and P. A. Wheeler (2003), Production and partitioning of organic matter during simulated phytoplankton blooms, *Limnol. Oceanogr. Methods*, *48*(5), 1808–1817.

Wetz, M. S., P. A. Wheeler, and R. M. Letelier (2004), Light-induced growth of phytoplankton collected during the winter from the benthic boundary later off Oregon, USA, *Mar. Ecol. Prog. Ser.*, *280*, 95–104.

Wilkerson, F. P., and R. C. Dugdale (1987), The use of large shipboard barrels and drifters to study the effects of coastal upwelling on phytoplankton dynamics, *Limnol. Oceanogr.*, *32*(2), 368–382.

Wilkerson, F. P., A. M. Lassiter, R. C. Dugdale, A. Marchi, and V. E. Hogue (2006), The phytoplankton bloom response to wind events and upwelled nutrients during the CoOP WEST study, *Deep Sea Res., Part II*, *53*(25-26), 3023–3048.